VII. D/Ja^2 used in (5.1) are 1.62, 0.790, and 0.596 times $[\frac{4}{3}S(S+1)]^{1/2}$ for the linear, square, and sc lattice, respectively. Fairly good agreement suggests the occurence of the spin diffusion also for the isotropic Heisenberg magnet of spin $S=\infty$ for the linear chain. As the convergence of the present expansion is similar for finite S and for the XY magnet of the square, sc, and bcc lattices, the spin diffusion may occur for these cases too. It is recalled that Gulley *et al.*[14] checked the spin diffusion constant previously given, in a similar way for the sc lattice.

Finally we compare our results with previous theoretical values. As mentioned in the Introduction, Mori and Kawasaki[1] essentially suggested to use formula (1.5) and to approximate $I(\vec{k}, t)$ for small k by a Gaussian distribution function. The second column [two term (Gaussian)] of Table V gives the values obtained by this method for the case of spin $\frac{1}{2}$. Those values are very good estimates to the values determined in the present work, which are listed at the last column of the same table. For large spins, the situation is not changed. The values obtained by Bennett and Martin[3] and Resibois and De Leener[2] are 20% less than the present values.

ACKNOWLEDGMENTS

The author is grateful to Professor E. R. Hunt and Dr. T. Horiguchi for valuable discussions. Computation was performed with the aid of computer IBM 360/44 of Computer Center, Ohio University.

*Senior foreign scientist of NSF and Ohio University (1971–1972). Present address: Department of Applied Science, Faculty of Engineering, Tohoku University, Sendai, Japan.

[1]H. Mori and K. Kawasaki, Progr. Theoret. Phys. (Kyoto) 27, 529 (1962).

[2]P. Resibois and M. De Leener, Phys. Rev. 152, 305 (1966); 152, 318 (1966); 178, 806 (1969); 178, 819 (1969).

[3]H. S. Bennett and P. C. Martin, Phys. Rev. 138, A608 (1965).

[4]T. Morita, J. Math. Phys. 12, 2062 (1971).

[5]T. Morita, J. Math. Phys. (to be published).

[6]H. Mori, Progr. Theoret. Phys. (Kyoto) 34, 399 (1965).

[7]T. Horiguchi and T. Morita (unpublished).

[8]T. Morita, J. Math. Phys. 13, 714 (1972).

[9]For example, see W. Magnus, F. Oberhettinger, and R. P. Soni, *Formulas and Theorems for the Special Functions of Mathematical Physics* (Springer-Verlag, Berlin, 1966).

[10]S. Katsura, T. Horiguchi, and M. Suzuki, Physica 46, 69 (1970).

[11]For example, see P. Mazur, Physica 43, 533 (1969); E. Barouch, B. M. McCoy, and M. Dresden, Phys. Rev. A2, 1075 (1970).

[12]J. R. Thompson, E. R. Hunt, and H. Meyer, Phys. Letters 25A, 313 (1967).

[13]C. G. Windsor, in *Neutron Inelastic Scattering*, Vol. II (IAEA, Vienna, 1968), p. 83.

[14]J. E. Gulley, D. Hone, D. J. Scalapino, and B. G. Silbernagel, Phys. Rev. B1, 1020 (1970).

PHYSICAL REVIEW B VOLUME 6, NUMBER 9 1 NOVEMBER 1972

Electronic Shielding of Pr^{3+} and Tm^{3+} Ions in Crystals*

Paul Erdös and Jack H. Kang†
Department of Physics, The Florida State University, Tallahassee, Florida 32306
(Received 22 February 1972)

The relativistic wave functions, the electronic shielding factors $\sigma_i (i=2,4,6)$, the quadrupole antishielding factors and quadrupole polarizabilities are calculated for Pr^{3+} and Tm^{3+} ions. Two different theoretical schemes, the variational and the outward-integration methods are used. The results are compared with each other and with experimental values derived mainly from Mössbauer spectroscopy.

I. INTRODUCTION

For the study of rare-earth and actinide ions in crystals a first estimate of the crystal field effect is often obtained by considering a bare crystal field reduced through shielding.[1] Other quantities of interest that are due to shielding are the nuclear quadrupole antishielding factor, as well as the quadrupole polarizability.

Two different schemes have been developed to deal with the shielding problem. One is a numerical integration method, the other a variational method. The aim of this paper is to compare the results of these two methods with each other in

two test cases, the Pr^{3+} and the Tm^{3+} ion.

The electronic configurations of these ions are $[Kr]4d^{10}4f^{2}5s^{2}5p^{6}$ and $[Kr]\,4d^{10}4f^{12}5s^{2}5p^{6}$, respectively. An *external* charge distribution will distort the electronic shells. The distorted charge distribution in these shells gives rise to an additional potential inside the ion. This is called "shielding." For instance, the unshielded crystal field V'_{4f} at the site of a $4f$ electron may always be expanded as

$$V'_{4f}=\sum_{l,m} A_l^m r^l Y_l^m(\theta,\phi)\ , \tag{1}$$

where $Y_l^m(\theta,\phi)$ are the normalized spherical harmonics, and A_l^m are constants determined by the external charge distribution (ions in the lattice). The spherical polar coordinates of the electron are r, θ, and ϕ; the angles being measured with respect to a set of mutually perpendicular axes fixed in the crystal. The radius is measured from the nucleus. In order to obtain the effective potential due to the shielding through the other electrons of the ion, it is customary to introduce the shielding factor σ_l, which measures the reduction of the crystal field parameter A_l^m. The shielded crystal field potential is then given by

$$V_{4f}=\sum_{l,m} A_l^m r^l(1-\sigma_l)\,Y_l^m. \tag{2}$$

Because of certain selection rules, only $l=2, 4$, and 6 occur, and the shielding factor σ_l is independent of the quantum number m.

This shielding effect for $4f$ electrons in the rare-earth ions has been estimated by Burns[2] and calculated both by Sternheimer[3] and Ray.[4] The former used the numerical-integration method and the latter the variational method to calculate the distorted wave functions by first-order perturbation theory. The shielding factor σ_2 in the Pr^{3+} ions has been found to be 0.67 by Sternheimer and 0.52 by Ray. However, in their first attempt, these authors calculated the shielding due to the $5s$ and $5p$ shells only. In later work,[5] Sternheimer *et al.* improved the calculation of σ_2, and calculated σ_4 and σ_6, by including the shielding through distortion of the $4s$, $4p$, and $4d$ shells. The effect of the further inner shells has not been calculated. The values of σ_4 and σ_6 were each found to be less than 0.1.

Both direct and exchange interaction between the $4f$ electrons and electrons in the other shells contribute to the shielding factors σ_l. The variational calculations up to date have only been carried out for the direct part of the shielding factor σ_2. The exchange part has been omitted. In this paper we want to give the results for all shielding factors σ_l ($l=2, 4, 6$), including direct as well as exchange contributions, and taking into account all shells. A slight generalization of the variational method, which may be useful for further investigations, will also be given. The calculation has been performed using recently obtained Slater-modified Hartree-Fock wave functions for the Pr^{3+} and Tm^{3+} ions.

II. SHIELDING OF $4f$ ELECTRON AND OF NUCLEUS

It has been demonstrated (Ref. 5, Sec. IV) how the combined effect of the crystal field and the electron-electron interaction upon the determinental wave function of the ion may be expressed in terms of the solutions $\Delta\psi(nl_im_i)$ of a single-electron perturbation problem. Therefore we will restrict our discussion to the latter, to explain the notation used to designate the various contributions to the shielding factors, and quadrupole antishielding and polarizability.

Because the crystal field potential is of the form (1), the shielding of each crystal field component,

$$H_1(l,m)=r^l A_l^m Y_l^m, \tag{3}$$

may be calculated separately.

Consider an electron whose wave function in the unperturbed ion with the Hamiltonian H_0 is

$$\psi^0(nl_im_i)=r^{-1}u^0(nl_i;\,r)\,Y_{l_i}^{m_i}(\theta,\phi)\ . \tag{4}$$

The external potential (3) adds a first-order correction to this wave function,

$$\Delta\psi(nl_im_i)=2A_l^m\sum_{lml_fm_f}\psi'(nl_im_i\rightarrow lm\rightarrow l_fm_f;\,\vec{r})\ , \tag{5}$$

with

$$\psi'(nl_im_i\rightarrow lm\rightarrow l_fm_f;\,\vec{r})=\frac{[(2l+1)(2l_i+1)]^{1/2}}{4\pi(2l_f+1)}\times\langle l_i0;\,l_f0\,|\,l_f0\rangle\langle l_im_i;\,lm\,|\,l_fm_f\rangle\times r^{-1}u'(nl_i\rightarrow l\rightarrow l_f;\,r)\,Y_{l_f}^{m_f}(\theta,\phi)\ . \tag{6}$$

The angle bracket symbols are the Clebsch-Gordan coefficients in the notation of Condon and Shortley.[6] The functions u' have to be determined in order to calculate the shielding factors. It is customary to consider these functions are arising from *radial excitations* if $l_f=l_i$. If $l_f\neq l_i$, one speaks of *angular excitations*.

The perturbational part $\Delta\psi$ of the wave function fulfills, in first order in $\Delta\psi$, the differential equation

$$(H_0-E^0_{nl_i})\,\Delta\psi(nl_im_i)=-[H_1(l,m)-E^1]\,\psi^0(nl_im_i)\ ; \tag{7}$$

therefore the angular factors of $H_1(l,m)\psi^0(nl_im_i)$ and of $\Delta\psi(nl_im_i)$ must be the same. This gives rise to the condition for l_f,

$$|l_i-l|\leq l_f\leq|l_i+l|\ . \tag{8}$$

Since $H_1(l,m)$ has even parity (l being even), $\Delta\psi$ and $\psi(nl_im_i)$ must have the same parity. This further restricts l_f as follows:

If l_i is even (odd), then l_f has to be even (odd). (9)

To ensure that the two sides of Eq. (7) have the same dependence on the azimuthal angle ϕ, the following condition must also hold:

$$m_f = m + m_i \,. \tag{10}$$

The shielding factor for $H_1(l, m)$ is written as a sum of direct and exchange parts

$$\sigma_l = \sigma_{lD} + \sigma_{lE} \,, \tag{11}$$

and each term of this sum is calculated as a sum of contributions from different excitations

$$\sigma_{lX} = \sum_{nl_il_f} \sigma_X(nl_i \to l \to l_f) \,, \quad X = D \text{ or } E \,. \tag{12}$$

These contributions are obtained by numerical integration of expressions (not given here) involving the unperturbed and perturbed wave function, and certain combinations of $3-j$ and $6-j$ symbols.[3,5]

The boundary conditions for the perturbed wave function are assumed to be the same as for the unperturbed wave function, i.e., that they vanish at infinity. It has been suggested[7] that if the perturbed wave function would be required to vanish at some finite distance from the nucleus, shielding parameters could be obtained which were in better agreement with experiment than the ones presently known. This "wave function in a box" approach would take cognizance of the repulsive effect of the ligand ion charge distributions.

Apart from the shielding factor, two other quantities of interest may be easily calculated once the wave function perturbed by the external charge distribution is known. These are the quadrupole antishielding factor γ_∞ and the quadrupole polarizability α_2. The former is defined through the equation

$$\left(\frac{\partial^2 V_{\text{eff}}}{\partial z^2}\right)_{r=0} = (1-\gamma_\infty)\left(\frac{\partial^2 V}{\partial z^2}\right)_{r=0} \,, \tag{13}$$

where V is the external potential and V_{eff} is the shielded potential at the nucleus. This quantity is of great interest, because its action on the nuclear quadrupole moment determines the nuclear quadrupole resonance frequency.

The quadrupole polarizability α_2 is the ratio of the quadrupole moment induced in the ion by an external charge (e.g., on the z axis) to the bare field gradient produced at the nucleus by the external charge:

$$-eQ_{zz} = \alpha_2 \left(\frac{\partial^2 V}{\partial z^2}\right)_{r=0} \,. \tag{14}$$

Here Q_{zz} is the relevant component of the ionic quadrupole moment tensor.

These quantities, expressed in terms of the wave functions, are[5,8]

$$\gamma_\infty = \sum_{l_il_f} C(l_i \to 2 \to l_f) \int_0^\infty u^0(l_i) u'(l_i \to 2 \to l_f)\, r^{-3}\, dr \,, \tag{15}$$

$$\alpha_2 = \sum_{l_il_f} C(l_i \to 2 \to l_f) \int_0^\infty u^0(l_i) u'(l_i \to 2 \to l_f)\, r^2\, dr \,. \tag{16}$$

Here,

$$C(l_i \to 2 \to l_f) = \tfrac{8}{5}(2l_i+1)(2l_f+1)\begin{pmatrix} l_f & 2 & l_i \\ 0 & 0 & 0 \end{pmatrix}^2$$

$$= \tfrac{8}{5}(2l_i+1)\langle l_i 0;\, 20 \mid l_f 0\rangle^2 \,. \tag{17}$$

Because of the factor r^{-3} in the integrand, the quadrupole shielding factor γ_∞ is very sensitive to the exact values of u' near $r=0$. In fact, the values obtained by (15) cannot be considered reliable (see Tables V and IX). Another formula[8] may be used (see Sec. V B), which does not suffer from this deficiency:

$$\gamma_\infty = \sum_{l_il_f} C(l_i \to 2 \to l_f) \int_0^\infty u^0(l_i)\, v'(l_i \to 2 \to l_f)\, r^2\, dr \,, \tag{18}$$

where $v'(r)$ is a solution of Eq. (31) with $l=-3$.

III. VARIATIONAL METHOD

In the determination of the perturbed wave functions the superposition principle allows to treat every occupied electronic level and every excitation separately. Therefore the subscripts nl_im_i and $nl_im_i \to l\,m \to l_fm_f$ will be dropped in the sequel.

The energy of the electron is written as

$$E = \frac{\langle \psi^0 + \Delta\psi \mid H_0 + H_1 \mid \psi^0 + \Delta\psi\rangle}{\langle \psi^0 + \Delta\psi \mid \psi^0 + \Delta\psi\rangle}$$

$$= E_0 + E_1 + \langle \Delta\psi \mid H_0 - E_0 \mid \Delta\psi\rangle + 2\langle \psi^0 \mid H_1 \mid \Delta\psi\rangle \,. \tag{19}$$

Using the expressions for ψ, $\Delta\psi$, and H_1 given in Sec. II, the energy reduces to

$$E = C_0 + C_1(\Phi_1 + \Phi_2) \,, \tag{20}$$

with

$$\Phi_1 = -2\int_0^\infty r^l u^0(r) u'(r)\, dr \,, \tag{21}$$

$$\Phi_2 = \int_0^\infty u'(r)\,(H_0 - E_0) u'(r)\, dr \,. \tag{22}$$

C_0 and C_1 are two constants. Here, H_0 is defined by $H_0 u^0 = E_0 u^0$:

$$H_0 = -\frac{d^2}{dr^2} + r^{-2}\hat{\mathbf{l}}^2 + V(r) \,, \tag{23}$$

where $\hat{\mathbf{l}}$ is the angular momentum operator, and $V(r)$ is the effective potential in which the electron moves.

The variational functions are chosen as multiples of the unperturbed function $u^0(nl_im_i)$. This choice allows one to evaluate all relevant integrals which occur in E analytically, and reduces the minimization problem to the solution of a set of linear equations for the variational parameters. *Herein lies the simplicity of the variational method as compared to the numerical-integration method.*

The choice of the polynomial factor of u^0 in the variational function u' is dictated by asymptotic conditions at $r=0$ as shown in Appendix A. The sums shown in the sequel extend from $n=0$ to a maximum N whose value is discussed below. The variational function for an angular excitation (i. e., for $l_i \neq l_f$) is chosen as

$$u' = r^{l+2} u^0 \sum a_n r^n \ . \tag{24}$$

The variational parameters are a_n. With this choice,

$$\Phi_1 = -2\sum a_n \langle r^{2l+n+2} \rangle \tag{25}$$

and

$$\Phi_2 = \sum_{m,n} a_m a_n [-l_i(l_i+1) + l_f(l_f+1) + (m+l+2)(n+l+2)] \langle r^{2l+m+n+2} \rangle \ . \tag{26}$$

Here

$$\langle r^p \rangle = \int_0^\infty (u^0)^2 r^p \, dr \ . \tag{27}$$

In the case of a radial excitation(i. e., for $l_i = l_f$) the orthogonality requirement between u' and u^0 has to be taken into account; hence, one chooses

$$u' = u^0 (r^2 \sum a_n r^n + f). \tag{28}$$

It follows that

$$f = -\sum a_n \langle r^{n+2} \rangle \ , \tag{29}$$

$$\Phi_1 = 2\sum a_n (\langle r^l \rangle \langle r^{n+2} \rangle - \langle r^{l+n+2} \rangle) \ ,$$

$$\Phi_2 = \sum_{m,n} a_m a_n (m+l+2)(n+l+2) \langle r^{m+n+2} \rangle \ . \tag{30}$$

We recall that there is a set of variational parameters for every type of excitation $nl_i m_i \rightarrow lm \rightarrow nl_f m_f$ allowed by the selection rules. They are now determined by minimizing $\Phi_1 + \Phi_2$ with respect to the variation of these parameters.

By the nature of the variational procedure one may include as many parameters as one wishes in the polynominal series and minimize the energy with respect to these parameters a_n. In the case of light ions it has been found[9] that two parameters are sufficient in the sense that the inclusion of more parameters does not further reduce the energy within the limits of computational accuracy.

Calculations reported in the literature have used both positive and negative powers of r in the power series multiplying u^0 in u'. As shown in Appendix A, the use of negative powers is incorrect. This explains why the use of more variational parameters gave worse results as compared to the numerical-integration method. This point will be further discussed in Sec. VI.

We have used ten variational parameters. The omission of the last one of these did not give any change in the resulting energy or shielding factors within the last significant digit given in the tables.

IV. NUMERICAL-INTEGRATION METHOD

It follows from (7), that the radial factor of the perturbational part of the wave function satisfies the differential equation[8]

$$\left(-\frac{d^2}{dr^2} + \frac{l_f(l_f+1)}{r^2} + V_0 - E_0\right) u'(r) = u^0(l_i m_i ; r)(r^l - \langle r^l \rangle \delta_{l_i l_f}) \ . \tag{31}$$

Here V_0 is the self-consistent potential used in the calculation of u^0. Hence $V_0 - E_0$ may be replaced by an expression containing u^0 [see Appendix A, Eq. (A3)]. If we denote by r_n a selected distance from the nucleus and by Δ the interval at the multiples of which u^0 is tabulated, the method of finite differences yields[8]

$$u'(r_{n+1}) = u'(r_n)\{2 + \Delta^2(l_f - l)(l_f + l + 1) r_n^{-2} + [u^0(r_{n+1}) - 2u^0(r_n) + u^0(r_{n-1})]/u^0(r_n)\} - u'(r_{n-1}) - \Delta^2 u^0(r_n)(r_n^l - \langle r^l \rangle \delta_{l l_f}) \ . \tag{32}$$

The wave function is given an arbitrary initial value $u'(r_1)$ at the smallest radius at which u^0 is known. Then the asymptotic condition

$$u'(r \rightarrow \infty) \propto e^{-(E_0)^{1/2} r} \tag{33}$$

is used to determine the correct value of $u'(r_i)$ by iterative, outward integration of (32).

V. RESULTS AND DISCUSSION

A. Shielding Factors

In order to make a meaningful comparison between these and previous results, it is necessary to note the difference of the unperturbed wave functions used in different claculations. Sternheimer[3] used Ridley[10] wave functions, obtained by a solution of the Hartree-equation. We used Lenander's method[11] to calculate the wave functions from a Slater-modified Hartree-Fock equation for both the variational and the numerical-integration method. The radial parts of these wave functions, which we denote by $u^0(r)$, are tabulated in Table I for Pr^{3+} and Tm^{3+}. As may be seen from Table II the differences between the two wave functions are not excessive. We tend to believe that the much more recent Lenander wave functions of Tm^{3+} and Pr^{3+} are of superior accuracy.

Computer programs have been developed by other authors[12] for the calculation of relativistic self-consistent Dirac-Slater wave functions, which are known[13] to yield considerably different values for $\langle r^2 \rangle$, $\langle r^4 \rangle$, and $\langle r^6 \rangle$ from the ones listed in Table II.

The perturbational corrections to all pertinent orbitals have been calculated and plotted, but are presented here in Figs. 1 and 2 merely for Pr^{3+}, and only for one radial and one angular excitation

TABLE I. Radial factor of the wave function of an electron in the outer nl shells of the Pr^{3+} and Tm^{3+} ions. The energy and the radius (r) are given in Rydbergs, and in units of $a_0 = 0.529 \times 10^{-8}$ cm, respectively. Four different radial intervals are used in the four sections of the table. Energies and wave functions for the 1S, 2S, 2P, 3S, 3P, 3D, 4S, 4P, and 4D inner shells do not generally differ very much from those for the neutral atom (Ref. 23) and are not shown, but they may be obtained from NAPS (Ref. 24).

Ion →	Pr^{3+}	Pr^{3+}	Pr^{3+}	Tm^{3+}	Tm^{3+}	Tm^{3+}
Shell →	5S	5P	4F	5S	5P	4F
Energy →	−4.606	−3.492	−2.662	−5.569	−4.101	−3.380
r	$U^0(r)$	$U^0(r)$	$U^0(r)$	$U^0(r)$	$U^0(r)$	$U^0(r)$
0.005	1.002×10^{-1}	9.211×10^{-3}	1.100×10^{-6}	1.187×10^{-1}	1.313×10^{-2}	3.175×10^{-6}
0.010	1.429×10^{-1}	3.169×10^{-2}	1.638×10^{-5}	1.576×10^{-1}	4.399×10^{-2}	4.669×10^{-5}
0.015	1.453×10^{-1}	6.129×10^{-2}	7.723×10^{-5}	1.446×10^{-1}	8.274×10^{-2}	2.175×10^{-4}
0.020	1.209×10^{-1}	9.345×10^{-2}	2.276×10^{-4}	1.004×10^{-1}	1.225×10^{-1}	6.335×10^{-4}
0.025	8.025×10^{-2}	1.249×10^{-1}	5.186×10^{-4}	4.037×10^{-2}	1.589×10^{-1}	1.427×10^{-3}
0.030	3.106×10^{-2}	1.535×10^{-1}	1.005×10^{-3}	-2.482×10^{-2}	1.888×10^{-1}	2.732×10^{-3}
0.035	-2.089×10^{-2}	1.776×10^{-1}	1.740×10^{-3}	-8.780×10^{-2}	2.108×10^{-1}	4.680×10^{-3}
0.040	-7.146×10^{-2}	1.965×10^{-1}	2.779×10^{-3}	-1.437×10^{-1}	2.242×10^{-1}	7.388×10^{-3}
0.045	-1.178×10^{-1}	2.095×10^{-1}	4.168×10^{-3}	-1.897×10^{-1}	2.289×10^{-1}	1.096×10^{-2}
0.050	-1.579×10^{-1}	2.167×10^{-1}	5.956×10^{-3}	-2.242×10^{-1}	2.252×10^{-1}	1.549×10^{-2}
0.055	-1.908×10^{-1}	2.182×10^{-1}	8.179×10^{-3}	-2.467×10^{-1}	2.141×10^{-1}	2.104×10^{-2}
0.060	-2.158×10^{-1}	2.142×10^{-1}	1.088×10^{-2}	-2.575×10^{-1}	1.963×10^{-1}	2.768×10^{-2}
0.065	-2.328×10^{-1}	2.053×10^{-1}	1.407×10^{-2}	-2.574×10^{-1}	1.727×10^{-1}	3.543×10^{-2}
0.070	-2.420×10^{-1}	1.918×10^{-1}	1.779×10^{-2}	-2.473×10^{-1}	1.446×10^{-1}	4.433×10^{-2}
0.075	-2.438×10^{-1}	1.745×10^{-1}	2.206×10^{-2}	-2.285×10^{-1}	1.128×10^{-1}	5.438×10^{-2}
0.080	-2.387×10^{-1}	1.538×10^{-1}	2.688×10^{-2}	-2.024×10^{-1}	7.847×10^{-2}	6.559×10^{-2}
0.085	-2.275×10^{-1}	1.303×10^{-1}	3.226×10^{-2}	-1.703×10^{-1}	4.237×10^{-2}	7.792×10^{-2}
0.090	-2.109×10^{-1}	1.046×10^{-1}	3.822×10^{-2}	-1.335×10^{-1}	5.403×10^{-3}	9.137×10^{-2}
0.095	-1.897×10^{-1}	7.728×10^{-2}	4.474×10^{-2}	-9.343×10^{-2}	-3.167×10^{-2}	1.059×10^{-1}
0.100	-1.645×10^{-1}	4.876×10^{-2}	5.183×10^{-2}	-5.114×10^{-2}	-6.819×10^{-2}	1.214×10^{-1}
0.105	-1.362×10^{-1}	1.955×10^{-2}	5.948×10^{-2}	-7.713×10^{-3}	-1.036×10^{-1}	1.380×10^{-1}
0.110	-1.054×10^{-1}	-9.922×10^{-3}	6.768×10^{-2}	3.588×10^{-2}	-1.373×10^{-1}	1.555×10^{-1}
0.115	-7.288×10^{-2}	-3.927×10^{-2}	7.641×10^{-2}	7.879×10^{-2}	-1.690×10^{-1}	1.738×10^{-1}
0.120	-3.918×10^{-2}	-6.816×10^{-2}	8.567×10^{-2}	1.203×10^{-1}	-1.983×10^{-1}	1.930×10^{-1}
0.125	-4.899×10^{-3}	-9.627×10^{-2}	9.543×10^{-2}	1.598×10^{-1}	-2.249×10^{-1}	2.129×10^{-1}
0.150	1.592×10^{-1}	-2.171×10^{-1}	1.511×10^{-1}	3.123×10^{-1}	-3.131×10^{-1}	3.216×10^{-1}
0.175	2.827×10^{-1}	-2.926×10^{-1}	2.163×10^{-1}	3.730×10^{-1}	-3.249×10^{-1}	4.396×10^{-1}
0.200	3.471×10^{-1}	-3.181×10^{-1}	2.879×10^{-1}	3.460×10^{-1}	-2.726×10^{-1}	5.596×10^{-1}
0.225	3.520×10^{-1}	-2.983×10^{-1}	3.630×10^{-1}	2.524×10^{-1}	-1.760×10^{-1}	6.757×10^{-1}
0.250	3.064×10^{-1}	-2.428×10^{-1}	4.392×10^{-1}	1.185×10^{-1}	-5.524×10^{-2}	7.838×10^{-1}
0.275	2.237×10^{-1}	-1.625×10^{-1}	5.144×10^{-1}	-3.150×10^{-2}	7.213×10^{-2}	8.109×10^{-1}
0.300	1.178×10^{-1}	-6.781×10^{-2}	5.867×10^{-1}	-1.785×10^{-1}	1.929×10^{-1}	9.656×10^{-1}
0.325	1.114×10^{-3}	3.218×10^{-2}	6.549×10^{-1}	-3.089×10^{-1}	2.980×10^{-1}	1.037×10^{0}
0.350	-1.158×10^{-1}	1.302×10^{-1}	7.181×10^{-1}	-4.141×10^{-1}	3.821×10^{-1}	1.095×10^{0}
0.375	-2.251×10^{-1}	2.207×10^{-1}	7.756×10^{-1}	-4.902×10^{-1}	4.427×10^{-1}	1.141×10^{0}
0.500	-5.232×10^{-1}	4.719×10^{-1}	9.730×10^{-1}	-4.584×10^{-1}	4.222×10^{-1}	1.212×10^{0}
0.625	-3.986×10^{-1}	3.872×10^{-1}	1.038×10^{0}	-3.701×10^{-2}	8.698×10^{-2}	1.125×10^{0}
0.750	-5.692×10^{-2}	1.176×10^{-1}	1.017×10^{0}	4.215×10^{-1}	-2.990×10^{-1}	9.865×10^{-1}
0.875	3.130×10^{-1}	-1.942×10^{-1}	9.502×10^{-1}	7.626×10^{-1}	-6.117×10^{-1}	8.418×10^{-1}
1.000	6.149×10^{-1}	-4.690×10^{-1}	8.626×10^{-1}	9.591×10^{-1}	-8.194×10^{-1}	7.094×10^{-1}
1.125	8.193×10^{-1}	-6.760×10^{-1}	7.707×10^{-1}	1.034×10^{0}	-9.306×10^{-1}	5.911×10^{-1}
1.250	9.309×10^{-1}	-8.114×10^{-1}	6.813×10^{-1}	1.024×10^{0}	-9.665×10^{-1}	4.904×10^{-1}
1.375	9.676×10^{-1}	-8.839×10^{-1}	5.978×10^{-1}	9.597×10^{1}	-9.493×10^{-1}	4.063×10^{-1}
1.500	9.498×10^{-1}	-9.061×10^{-1}	5.218×10^{-1}	8.667×10^{-1}	-8.976×10^{-1}	3.364×10^{-1}
1.625	8.961×10^{-1}	-8.908×10^{-1}	4.538×10^{-1}	7.619×10^{-1}	-8.259×10^{-1}	2.787×10^{-1}
1.750	8.210×10^{-1}	-8.496×10^{-1}	3.936×10^{-1}	6.565×10^{-1}	-7.445×10^{-1}	2.310×10^{-1}
1.875	7.357×10^{-1}	-7.918×10^{-1}	3.408×10^{-1}	5.571×10^{-1}	-6.605×10^{-1}	1.918×10^{-1}
2.000	6.479×10^{-1}	-7.246×10^{-1}	2.947×10^{-1}	4.673×10^{-1}	-5.786×10^{-1}	1.595×10^{-1}
2.625						
2.625	2.884×10^{-1}	-3.933×10^{-1}	1.361×10^{-1}	1.665×10^{-1}	-2.598×10^{-1}	6.088×10^{-2}
3.250	1.088×10^{-1}	-1.809×10^{-1}	6.078×10^{-1}	5.194×10^{-2}	-1.023×10^{-1}	2.286×10^{-2}
3.875	4.027×10^{-2}	-8.017×10^{-2}	2.786×10^{-2}	1.635×10^{-2}	-3.997×10^{-2}	9.032×10^{-3}
4.500	1.359×10^{-2}	-3.247×10^{-2}	1.211×10^{-2}	4.737×10^{-3}	-1.438×10^{-2}	3.395×10^{-3}
5.125	4.306×10^{-3}	-1.244×10^{-2}	5.100×10^{-3}	1.286×10^{-3}	-4.891×10^{-3}	1.233×10^{-3}

TABLE II. Comparison of the means of different powers of the atomic radius in atomic units of the $4f$ electron in Pr^{3+} and Tm^{3+} ions. Sternheimer used Freeman and Watson's $\langle r^2\rangle_{4f}$ calculated from Hartree-Fock wave functions (given as 1.086). He also used $\langle r^4\rangle_{4f}$ and $\langle r^6\rangle_{4f}$ calculated from Ridley's Hartree wave functions. In this work the mean radius of the $4f$ wave function was generated from Lenander's computer program for Slater-modified Hartree-Fock wave functions.

	Pr^{3+}			Tm^{3+}		
	Freeman and Watson	Ridley	Lenander	Freeman and Watson	Ridley	Lenander
$\langle r^2\rangle_{4f}$	1.086		1.099	0.646		0.6220
$\langle r^4\rangle_{4f}$	2.822	2.839	2.834		1.068	0.9687
$\langle r^6\rangle_{4f}$	15.726	16.017	14.419		3.653	3.2133

for each method of solution, and for external and internal perturbations, respectively.

The perturbational parts $u'(r)$ of the wave function arising from the external radial excitation $5p \rightarrow 2 \rightarrow p$ are plotted in Figs. 1(a) and 1(b); those arising from the external angular excitation $5p \rightarrow 2 \rightarrow f$ are plotted in Figs. 1(c) and 1(d). These are calculated by the numerical [1(a) and 1(c)] and variational [1(b) and 1(d)] methods, respectively. Also shown on each figure is the unperturbed $5p$ function $u^0(r)$. The scale of the abscissa is not arbitrary but is determined by the magnitude of

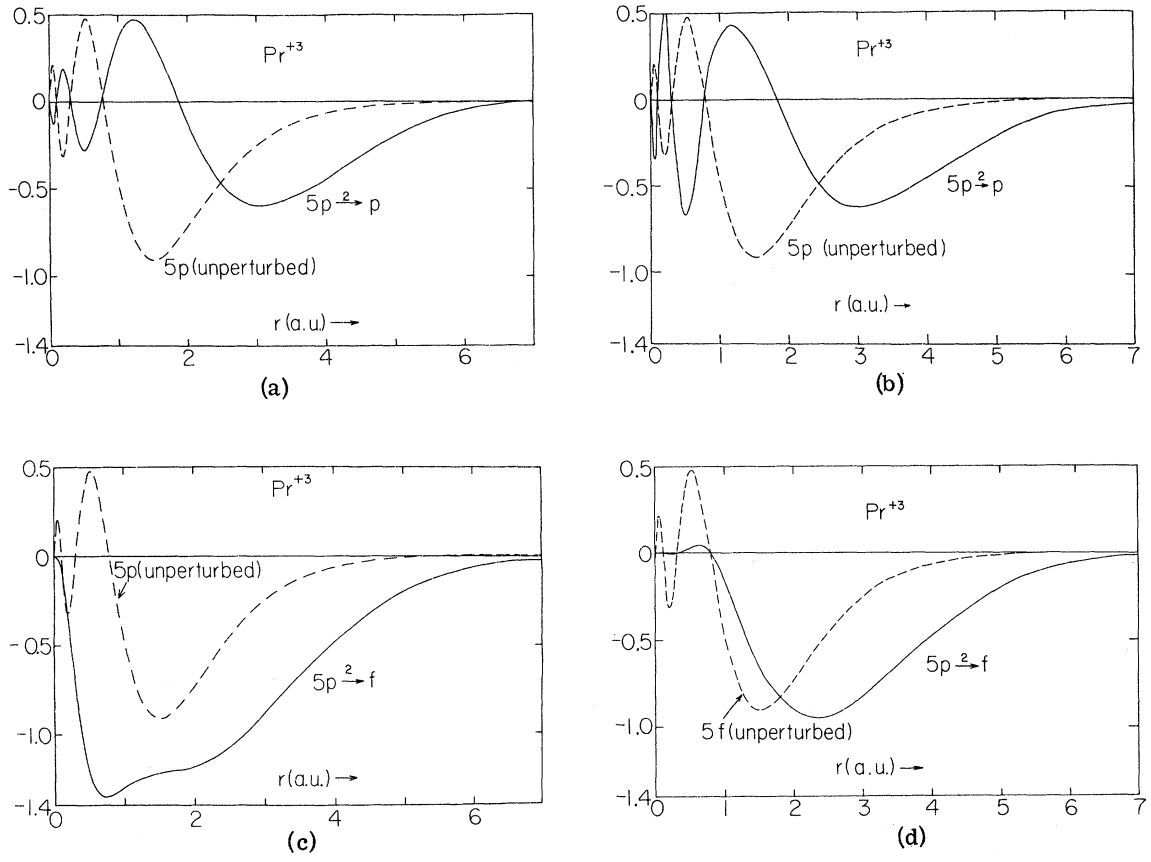

FIG. 1. Radial factor $u^0(5p0)$ of an unperturbed wave function of Pr^{3+}, together with the first-order perturbational correction $u'(5p0 \rightarrow 2 \rightarrow p0)$ shown in (a) and (b), and $u'(5p0 \rightarrow 2 \rightarrow f0)$ shown in (c) and (d), due to the $l=2$, $m=0$ spherical harmonic component of an *external* potential. Compare diagrams on left and right to collate the results of the numerical integration with those obtained by the variational principle. Compare diagrams at top and bottom to see the effects of radial and angular excitations.

$u^0(r)$ through the inhomogeneous differential Eq. (31). It should not be disturbing that the perturbed part of the wave function appears to be as big as the unperturbed wave function: As long as $A_l^m \ll 1$, Eq. (5) ensures that the total perturbational function $\Delta\psi$ is small compared to ψ^0.

Figures 1(a) and 1(b) show, that for the radial excitation the two methods lead to very similar wave functions. Since the excitation has the same angular momentum quantum number as the unperturbed state, they have the same number of nodes. In addition, the nodes of the two functions essentially coincide with those of the unperturbed function. The numerical wave function in 1(a) is noticeably smaller at small radii (within the first two nodes) than its variational counterpart.

Figures 1(c) and 1(d) show considerable differences between the wave functions of angular excitations obtained by the numerical-integration and variational method. The nodes forced on the variational function at the nodes of the unperturbed function completely alter the behavior of $u'(r)$ for $r < 3$ a.u. The numerical function has no nodes at all. We believe that the variational function does not correctly reproduce the effect of the perturbation, because it forces the perturbed wave function to have nodes where the unperturbed wave function has its nodes.

These properties of the wave functions are reflected in the shielding factors, as discussed below.

Apart from the excitations arising from $H_1(l, m)$ [Eq. (3)], with $l > 0$, we also calculated wave functions $v'(r)$ for excitations with $l < 0$. These are needed to evaluate Eq. (18). Their significance is elaborated in Appendix B. A representative set of these functions is plotted in Figs. 2(a)–2(d).

The results for the shielding factors are presented in tabular form. All entries under the heading "Sternheimer numerical integration" are taken from the references cited below under the name of this author.

Tables III–V present the contributions to the shielding factors arising from the different excitations in Pr^{3+}, Tables VI–VIII show the corresponding results for Tm^{3+}.

The calculations have been carried out not only for the excitation shown in the tables, but for all inner shells as well. It was found, however, that the contribution to σ_k of each of these excitations, ranging from $1s \rightarrow d$ to $3d \rightarrow g$, was less than 0.001. These small, but numerous, contributions of the inner shells have been included in the cumulative results of Tables IX and X.

The most conspicuous features of these results are the following.

There is a general agreement with respect to order of magnitude and sign of the three values obtained for each entry in the table. This indicates that all three calculations are free from basic errors.

We see from Tables III and VI, that the *two sets of results obtained by numerical integration* for $\sigma_2(nl_i \rightarrow l_f)$ are close. The two largest contributions $5p \rightarrow f$ and $5s \rightarrow d$ agree within 6%. The $5p \rightarrow p$ contributions differ by ~35%. Although we are unable to tell why some contributions differ more than others, the general trend seems to be that the radial excitations (which give antishielding, thus negative contributions) differ more than the angular excitations.

On the other hand, the *differences between the results obtained by the variational and numerical-integration methods* are considerable in particular in the case of the most important $5p \rightarrow f$ contribution (35%). These differences arise from the differences of the perturbational part of the wave function, which is shown in Figs. 1(c) and 1(d). As has been noted earlier, the variational ansatz forces $u'(r)$ to have nodes everywhere where $u^0(r)$ has nodes, whereas the nodes of the true wave function may be located elsewhere. The resulting distortion of the shielding charge distribution from the actual one seems to give rise to the large differences in the shielding factors. In contrast to this, the radial excitation $5p \rightarrow 2 \rightarrow p$ gives rise to close values of σ_2 obtained by the numerical and variational methods. This reflects the fact noted above, that the radial wave functions do not differ substantially.

The summaries in Tables IX and X show that σ_2 as calculated by the integration method may be considered as correct probably within 5%, whereas the variational value should be taken only as indicative.

For σ_4 the situation is less favorable: Here the direct and exchange contributions to the shielding factor almost cancel, so that the deviations in the results of the two numerical integrations, which are of the order of 10%, make the final results in Tables IX and X differ by a factor of 3.

This is not very serious, because σ_4 is less than 0.1, and therefore the crystal field reduction factor $1 - \sigma_4$, e.g., for Pr^{3+}, is 0.97 or 0.91, respectively.

Best concurrence between the three results is observed for σ_6. Here the exchange shielding is larger than the direct shielding by a factor of 2; therefore the cancellation observed in σ_4 does not occur.

B. Quadrupole Antishielding Factors and Quadrupole Polarizabilities

We have used two different methods to calculate the quadrupole antishielding factor γ_∞. One method determines the perturbative correction u' to the wave function due to the quadrupole moment

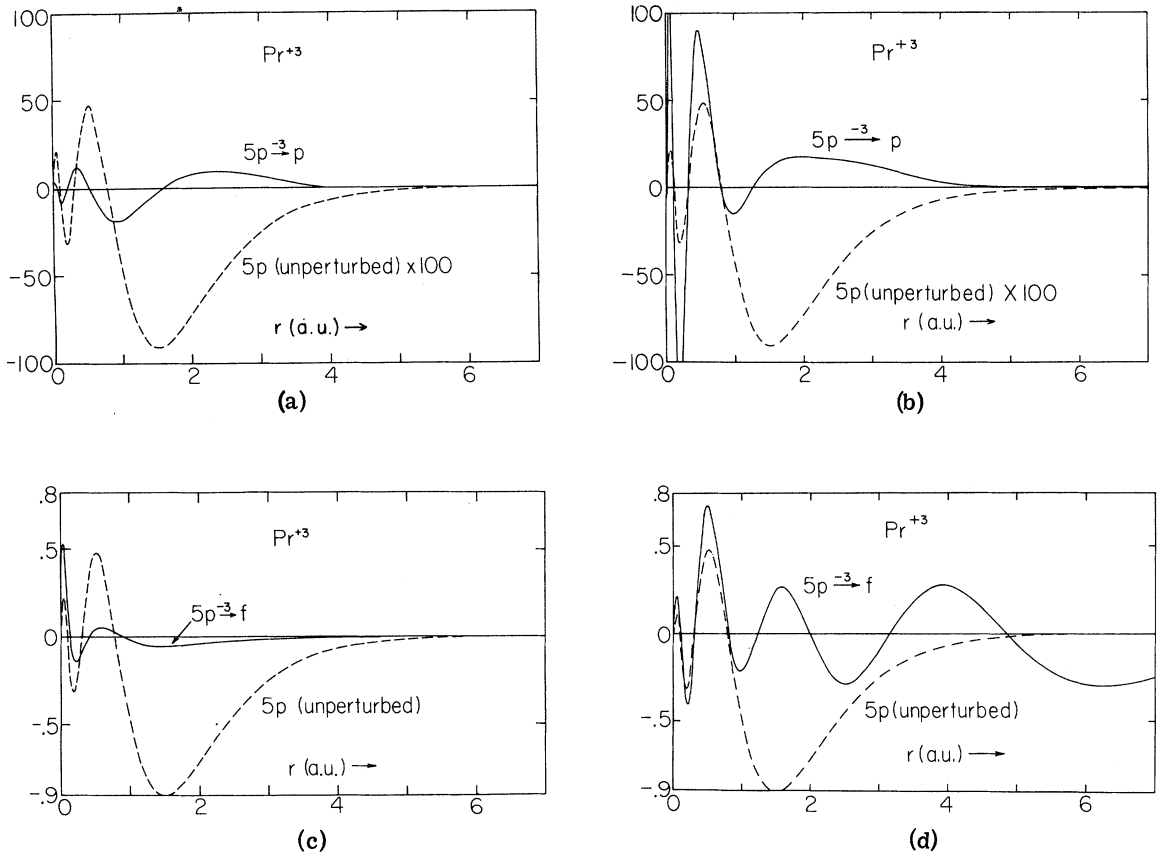

FIG. 2. Radial factor $u^0(5p0)$ of an unperturbed wave function of Pr^{3+} together with the first-order perturbational correction $u'(5p0 \rightarrow -3 \rightarrow p0)$ shown in (a) and (b), and $u'(5p0 \rightarrow -3 \rightarrow f0)$ shown in (c) and (d) due to the $l=-3$, $m=0$ spherical harmonic component of an *internal* (nuclear quadrupole) potential. Compare diagrams on left and right to collate the results of the numerical integration with those obtained by the variational principle. Compare diagrams at top and bottom to see the effects of radial and angular excitations.

TABLE III. Contributions to the shielding factor σ_2 of the $4f$ electron in Pr^{3+}.

Excitation	Direct shielding factor σ_D			Exchange shielding factor σ_E		
$nl_i \rightarrow l_f$	Variational principle	Numerical integration	Sternheimer numerical integration	Variational principle	Numerical integration	Sternheimer numerical integration
$5s \rightarrow d$	0.3127	0.2834	0.2895	−0.0544	−0.0455	−0.0361
$5p \rightarrow p$	−0.1805	−0.1444	−0.1873	−0.0387	0.0342	0.0427
$5p \rightarrow f$	0.4135	0.5825	0.5759	−0.0619	−0.1076	−0.0817
$4s \rightarrow d$	0.0319	0.0382	0.0356	−0.0088	−0.000	−0.0096
$4p \rightarrow p$	−0.0001	−0.0014	−0.0018	−0.0012	−0.0004	−0.0005
$4p \rightarrow f$	0.0407	0.0481	0.0493	−0.0111	−0.0133	−0.0134
$4d \rightarrow s$	−0.0379	−0.0340	−0.0375	0.0094	0.0079	0.0084
$4d \rightarrow d$	−0.0043	−0.0060	−0.0075	−0.0031	−0.0007	−0.0006
$4d \rightarrow g$	0.0551	0.0563	0.0611	−0.0142	−0.0146	−0.0155
$3s \rightarrow d$	0.0009	0.0015		−0.0002	−0.0003	
$3p \rightarrow p$	0.0002	0.0002		−0.0001	−0.0001	
$3p \rightarrow f$	0.0010	0.0011		−0.0002	−0.0002	
$3d \rightarrow s$	0.0002	−0.0010		−0.0001	0.0001	
$3d \rightarrow d$	0.0003	0.0003		−0.0003	−0.0003	
$3d \rightarrow g$	0.0008	0.0008		−0.0002	−0.0002	
Total	0.6346	0.8254	0.7778	−0.1078	−0.1512	−0.1063

TABLE IV. Contributions to the shielding factor σ_4 of a $4f$ electron in Pr^{3+}.

Excitation	Direct shielding factor σ_D			Exchange shielding factor σ_E		
$nl_i \rightarrow l_f$	Variational principle	Numerical integration	Sternheimer numerical integration	Variational principle	Numerical integration	Sternheimer numerical integration
$5s \rightarrow g$	0.0366	0.0392	0.0436	−0.0218	−0.0236	−0.0248
$5p \rightarrow f$	0.1317	0.1964	0.2128	−0.1090	−0.2093	−0.1820
$5p \rightarrow h$	0.0576	0.0597	0.0700	−0.0260	−0.0271	−0.0288
$4s \rightarrow g$	0.0012	0.0013		−0.0010	−0.0011	
$4p \rightarrow f$	0.0034	0.0041		−0.0043	−0.0051	
$4p \rightarrow h$	0.0018	0.0019		−0.0013	−0.0013	
$4d \rightarrow d$	−0.0023	−0.0026	−0.0028	−0.0007	0.0000	−0.0003
$4d \rightarrow g$	0.0040	0.0043	0.0048	−0.0084	−0.0087	−0.0100
$4d \rightarrow i$	0.0031	0.0031	0.0035	−0.0016	−0.0016	−0.0018
$3s \rightarrow g$	0.0	0.0		−0.0	−0.0	
$3p \rightarrow f$	0.0	0.0		−0.0	−0.0	
$3p \rightarrow h$	0.0	0.0		−0.0	−0.0	
$3d \rightarrow d$	0.0	0.0		−0.0	−0.0	
$3d \rightarrow g$	0.0	0.0		−0.0	−0.0	
$3d \rightarrow i$	0.0	0.0		−0.0	−0.0	
Total	0.2374	0.3075	0.3318	−0.1742	−0.2779	−0.2470

of the charge distribution from Eq. (31), with $l = 2$, and uses Eq. (15) for γ_∞. The second method finds the perturbative correction v' to the wave function due to the nuclear quadrupole moment from Eq. (31) with $l = -3$, and uses Eq. (18) for γ_∞.

The quadrupole antishielding factors obtained by the first and second method will be denoted by the adjectives "external" and "nuclear," respectively. They are listed in Tables XI and XII for the ions Pr^{3+} and Tm^{3+}, together with the values previously obtained by Sternheimer in Ref. 3.

It has been proven by Sternheimer and Foley that in theory, the two methods give the same results for γ_∞ in first-order perturbation theory. In practice, the two results often differ, because the perturbational corrections to the wave function are not accurately calculated.

Care has to be exercised in connection with the interpretation of Sternheimer's statement, that the two quadrupole antishielding factors so obtained are equal in second order. Second order perturbation theory usually means calculating the wave function and the energy from the Schrödinger equation up to terms in second order in the perturbing potential. Instead of this, the cited author determines the perturbed wave function from the first-order perturbation and Eq. (31), where the

TABLE V. Contributions to the shielding factors σ_6 of a $4f$ electron in Pr^{3+}.

Excitation	Direct shielding factor σ_D			Exchange shielding factor σ_E		
$nl_i \rightarrow l_f$	Variational principle	Numerical integration	Sternheimer numerical integration ratios	Variational principle	Numerical integration	Sternheimer numerical principle integration
$5s \rightarrow i$	0.0061	0.0064	0.0066	−0.0094	−0.-097	−0.0099
$5p \rightarrow h$	0.0211	0.0230	0.0265	−0.0533	−0.0567	−0.0649
$5p \rightarrow j$	0.0117	0.0117	0.0130	−0.0104	−0.0105	−0.0113
$4s \rightarrow i$	0.0001	0.0001		−0.0001	−0.0001	
$4p \rightarrow h$	0.0002	0.0002		−0.0006	−0.0006	
$4p \rightarrow j$	0.0001	0.0001		−0.0001	−0.0001	
$4d \rightarrow g$	0.0007	0.0008		−0.0060	−0.0065	
$4d \rightarrow i$	0.0003	0.0003		−0.0005	−0.0005	
$4d \rightarrow k$	0.0002	0.0002		−0.0002	−0.0002	
Total	0.0404	0.0428	0.0461	−0.0806	−0.0850	−0.0861

TABLE VI. Contributions to the shielding factor σ_2 of a $4f$ electron in Tm^{3+}.

Excitation	Direct shielding factor σ_D			Exchange shielding factor σ_E		
$nl_i \rightarrow l_f$	Variational principle	Numerical integration	Sternheimer numerical integration	Variational principle	Numerical integration	Sternheimer numerical integration
$5s \rightarrow d$	0.2951	0.2937	0.2737	−0.0447	−0.0434	−0.0335
$5p \rightarrow p$	−0.2209	−0.1779	−0.2401	0.0459	0.0387	0.0453
$5p \rightarrow f$	0.3836	0.4625	0.5001	−0.0490	−0.0643	−0.0618
$4s \rightarrow d$	0.0330	0.0422	0.0395	−0.0090	−0.0114	−0.0104
$4p \rightarrow p$	−0.0012	−0.0016	−0.0026	−0.0080	−0.0002	0.0024
$4p \rightarrow f$	0.0405	0.0493	0.0458	−0.0109	−0.0136	−0.0124
$4d \rightarrow s$	−0.0388	−0.0420	−0.0395	0.0100	0.0104	0.0094
$4d \rightarrow d$	−0.0058	−0.0062	0.0078	−0.0013	0.0004	0.0016
$4d \rightarrow g$	0.0505	0.0518	0.0498	−0.0129	−0.0132	−0.0125
$3s \rightarrow d$	0.0011	0.0020		−0.0002	−0.0004	
$3p \rightarrow p$	0.0003	0.0002		−0.0001	−0.0001	
$3p \rightarrow f$	0.0012	0.0012		−0.0003	−0.0003	
$3d \rightarrow s$	0.0002	−0.0014		−0.0001	−0.0002	
$3d \rightarrow d$	0.0003	0.0003		−0.0003	−0.0003	
$3d \rightarrow g$	0.0009	0.0009		−0.0002	−0.0002	
Total	0.5398	0.6748	0.6189	−0.0739	−0.0976	−0.0741

right-hand side is multiplied by a factor which represents the effective potential due to the charge distribution and its first-order induced moment.

It will be shown in Appendix B that in the variational calculation the external and nuclear methods (using u' and v', respectively) also give the same results with the additional feature, that even in practice the numerical results are equal up to the last significant digit which may be obtained in the solution of a set of linear equations of order N, where N is the number of variational parameters used. Therefore, the tables contain only one set of variational values in contrast to the two sets of values of $\gamma_{\infty ext}$ and $\gamma_{\infty nucl}$ obtained from the numerical solution of the differential equation.

Again, the conclusion is, that the values obtained by the variational calculation should not be considered as reliable as the ones calculated by numerical integration. The tables show that sizable contributions arise from the shells not considered by previous authors. We consider the nuclear values of γ_∞ the best, because they are not so sensitive to uncertainties in the wave function close to $r = 0$.

TABLE VII. Contributions to the shielding factor σ_4 of a $4f$ electron in Tm^{3+}.

Excitation	Direct shielding factor σ_D			Exchange shielding factor σ_E		
$nl_i \rightarrow l_f$	Variational principle	Numerical integration	Sternheimer numerical integration	Variational principle	Numerical integration	Sternheimer numerical integration
$5s \rightarrow g$	0.0368	0.0398	0.0409	−0.0202	−0.0220	−0.0223
$5p \rightarrow f$	0.1298	0.1608	0.1926	−0.0992	−0.1632	−0.1629
$5p \rightarrow h$	0.0562	0.0592	0.0652	−0.0231	−0.0245	−0.0259
$4s \rightarrow g$	0.0014	0.0014		−0.0012	−0.0012	
$4p \rightarrow f$	0.0037	0.0046		−0.0046	−0.0056	
$4p \rightarrow h$	0.0020	0.0020		−0.0013	−0.0014	
$4d \rightarrow d$	−0.0029	−0.0031		0.0006	0.0012	
$4d \rightarrow g$	0.0038	0.0041		−0.0078	−0.0082	
$4d \rightarrow i$	0.0029	0.0029		−0.0014	−0.0014	
$3s \rightarrow g$	0.0000	0.0000		−0.0000	−0.0000	
$3p \rightarrow f$	0.0000	0.0000		−0.0000	−0.0000	
$3p \rightarrow h$	0.0000	0.0000		−0.0000	−0.0000	
$3d \rightarrow d$	0.0000	0.0000		−0.0000	−0.0000	
$3d \rightarrow g$	0.0000	0.0000		−0.0000	−0.0000	
$3d \rightarrow i$	0.0000	0.0000		−0.0000	−0.0000	
Total	0.2337	0.2719	0.2987	−0.1582	−0.2265	−0.2112

TABLE VIII. Contributions to the shielding factor σ_6 of a $4f$ electron in Tm^{3+}.

Excitation	Direct shielding factor σ_D			Exchange shielding factor σ_E		
$nl_i \rightarrow l_f$	Variational principle	Numerical integration	Sternheimer numerical integration	Variational principle	Numerical integration	Sternheimer numerical integration
$5s \rightarrow i$	0.0061	0.0067	0.0071	−0.0090	−0.0097	−0.1106
$5p \rightarrow h$	0.0217	0.0245	0.0294	−0.0533	−0.0581	−0.0713
$5p \rightarrow j$	0.0118	0.0120	0.0143	−0.0100	−0.0102	−0.0121
$4s \rightarrow i$	0.0001	0.0001		−0.0001	−0.0001	
$4p \rightarrow h$	0.0002	0.0002		−0.0007	−0.0007	
$4p \rightarrow h$	0.0001	0.0001		−0.0001	−0.0001	
$4d \rightarrow g$	0.0006	0.0007		−0.0054	−0.0059	
$4d \rightarrow i$	0.0002	0.0002		−0.0004	−0.0004	
$4d \rightarrow k$	0.0002	0.0002		−0.0002	−0.0002	
Total	0.0410	0.0448	0.0508	−0.0794	−0.0855	−0.0940

The same remarks hold also for the quadrupole polarizability of the ions in question, displayed in Tables XIII and XIV. In the case of Pr^{3+}, our value 57.27 is considerably larger than the present value 41.28 in the literature. This is not due to the contribution of shells neglected previously, but to large differences in the $5s \rightarrow d$, $5p \rightarrow p$, and $5p \rightarrow f$ contributions.

In summary we draw the following conclusions.

The numerical integration method is quantitatively more reliable for calculations of the shielding factor than the present form of the variational method.

Another variational ansatz, such as

$$u'(r) = e^{-E_0^{1/2} r} P(r) ,$$

with $P(r)$ a polynomial may give more satisfactory results. This would, however, deprive the variational method of its great advantage which results setting u' proportional to u^0. In that case no numerical integration had to be carried out in calculating the energy since all integrals reduced to the form $\int (u^0)^2 r^n dr = \langle r^n \rangle$.

The second conclusion is that the present state of the art allows a calculation of the factors $(1-\sigma_l)$ with an estimated accuracy of roughly 5%. Based on a comparison of the nuclear and external quadrupole antishielding factors (which should be equal), we estimate the accuracy of this factor and of the quadrupole polarizability as 10%.

VI. COMPARISON WITH EXPERIMENTAL RESULTS

The shielding of the external (crystal) potential and of the internal (nuclear quadrupole) potential plays an important role in many experiments, notably in nuclear alignment, nuclear magnetic resonance, Mössbauer effect, optical (luminescence) spectroscopy, magnetic susceptibility, etc. None of these experiments enables one to determine the shielding factors σ_l or the antishielding factors γ_∞ independently. For instance, by studying the temperature dependence of the nuclear quadrupole splitting of Tm^{3+} by recoilless nuclear resonance absorption, the ratio $(1-\gamma_\infty)/(1-\sigma_2)$ was determined for $Tm(C_2H_5SO_4)_3 \cdot 9H_2O$ and Tm_2O_3,[14] and for the hexagonal intermetallic compounds $TmRu_2$, $TmRe_2$, and $TmMn_2$.[15] In all of these compounds the rare-earth ions are at sites with lower than cubic symmetry. This gives rise to a crystal field component of the type $A_2(1-\sigma_2)$ [cf. Eq. (2)]. In compounds, where the site symmetry is cubic, the term involving σ_2 is absent, and only σ_4 and σ_6 appear. Since the latter shielding factors are much smaller than σ_2, the inaccuracy of the experiments[16] does not allow conclusions about σ_4 and σ_6, or, from an opposite point of view, σ_4 and σ_6 are not needed to interpret the experimental results

TABLE IX. Summary of the results for the shielding factors σ_l of a $4f$ electron in Pr^{3+}.

σ_l	Variational principle	Numerical integration (this work)	Sternheimer numerical integration
σ_2	0.5391	0.6667	0.0672
σ_4	0.0643	0.0272	0.091
σ_6	−0.0403	−0.0421	−0.040

TABLE X. Summary of the results for the shielding factors σ_l of a $4f$ electron in Tm^{3+}.

σ_l	Variational principle	Numerical integration (this work)	Sternheimer numerical integration
σ_2	0.4659	0.5772	0.545
σ_4	0.0755	0.0454	0.088
σ_6	−0.0384	−0.0407	−0.043

TABLE XI. Quadrupole antishielding factor of Pr^{3+}.

Excitation	External			Nuclear	
$nl_i \rightarrow l_f$	Variational principle	Numerical integration	Sternheimer numerical integration	Numerical integration	Sternheimer numerical integration
$5s \rightarrow d$	0.5521	0.1374	0.566	0.1561	−69.7
$5p \rightarrow p$	−143.3075	−54.6081	−73.7	−54.4924	
$5p \rightarrow f$	0.6289	0.5224	0.515	0.5229	
$5s \rightarrow d$	0.2421	0.0812		0.0851	
$4p \rightarrow p$	−25.7773	−8.0535		−10.7758	−8.81
$4p \rightarrow f$	0.2561	0.1719		0.1719	
$4d \rightarrow s$	−0.5836	0.0363		0.0268	
$4d \rightarrow d$	−5.8406	−2.5909		−2.8901	−2.83
$4d \rightarrow g$	0.2600	0.2303		0.2302	
$3s \rightarrow d$	0.1056	0.0458		0.0465	
$3p \rightarrow p$	−4.0670	−1.4082		−1.6946	−1.545
$3p \rightarrow f$	0.1039	0.0795		0.0795	
$3d \rightarrow s$	−0.2794	−0.0123		−0.0132	
$3d \rightarrow d$	−0.3162	−0.3113		−0.3249	−0.322
$3d \rightarrow g$	0.0861	0.0897		0.0898	
Total	−177.9367	−65.5897	−72.619	−68.7422	−80.9

within the limits of accuracy. Magnetic susceptibility measurements in cubic compounds, even if they are of high accuracy[17] do not lend themselves to a determination of σ_4 and σ_6, because the core crystal field parameters A_4^m and A_6^m cannot be calculated by any present model even to an accuracy of the order of σ_4 or σ_6.

We therefore concentrate on the ratio $(1-\gamma_\infty)/(1-\sigma_2)$, which was determined as explained above.[14,15] The quadrupole splitting, which is directly measured, is given by

$$\langle \Delta E\rangle_T = \frac{e^2Q}{2}\Bigg[\Bigg(\langle J\|\alpha\|J\rangle(1-R_Q)\langle r^{-3}\rangle_{4f}\langle 3J_R^2 - J^2\rangle_T + \frac{4A_2^0}{e^2\langle r^2\rangle_{4f}}\frac{1-\gamma_\infty}{1-\sigma_2}\Bigg)^2 + \frac{1}{3}\Bigg(\frac{3}{2}\langle J\|\alpha\|J\rangle(1-R_Q)\langle r^{-3}\rangle_{4f}\langle J_+^2 + J_-^2\rangle_T + \frac{4A_2^2}{e^2\langle r^2\rangle_{4f}}\frac{1-\gamma_\infty}{1-\sigma_2}\Bigg)^2\Bigg]^{1/2}. \quad (34)$$

Here Q is the nuclear quadrupole moment,

TABLE XII. Quadrupole antishielding factor of Tm^{3+}.

Excitation	External			Nuclear	
$nl_i \rightarrow l_f$	Variational principle	Numerical integration (this work)	Sternheimer numerical integration	Numerical integration (our values)	Sternheimer numerical integration
$5s \rightarrow d$	0.46	0.18	0.468	0.19	
$5p \rightarrow p$	−121.87	−50.85	−65.5	−52.29	−67.2
$5p \rightarrow f$	0.53	0.49	0.491	0.50	
$4s \rightarrow d$	0.20	0.07		0.07	
$4p \rightarrow p$	−20.70	−6.21		−9.21	−6.79
$4p \rightarrow f$	0.21	0.14		0.14	
$4d \rightarrow s$	−0.47	−0.04		0.03	
$4d \rightarrow d$	−4.52	−1.98		−2.39	−2.18
$4d \rightarrow g$	0.20	0.18		0.18	
$3s \rightarrow d$	0.09	0.04		0.04	
$3p \rightarrow p$	−3.31	−1.12		−1.37	−1.18
$3p \rightarrow f$	0.09	0.06		0.06	
$3d \rightarrow s$	−0.22	−0.01		−0.01	
$3d \rightarrow d$	−0.23	−0.23		−0.25	
$3d \rightarrow g$	0.07	0.07		0.07	
Total	−149.47	−59.12	−64.541	−64.23	−75.3

TABLE XIII. Quadrupole polarizability of Pr^{3+} in a.u. $(0.5292\ \text{Å})^5$.

Excitation $nl_i \rightarrow l_f$	Variational principle	Numerical integration	Sternheimer numerical integration
$5s \rightarrow d$	12.28	10.89	7.23
$5p \rightarrow p$	8.01	7.28	6.58
$5p \rightarrow f$	30.12	38.40	27.47
$5s \rightarrow p$	0.08	0.09	
$4p \rightarrow p$	0.03	0.03	
$4p \rightarrow f$	0.12	0.14	
$4d \rightarrow s$	0.06	0.08	
$4d \rightarrow d$	0.10	0.09	
$4d \rightarrow g$	0.27	0.27	
Total	51.09	57.27	41.28

$\langle J \| \alpha \| J \rangle$ are the reduced matrix elements (for Tm^{3+} including an intermediate-coupling correction), R_Q is the atomic $(4f)$ Sternheimer shielding factor, and the brackets $\langle \cdots \rangle_T$ denote the thermal average of the expectation values of the angular momentum of the ion, in different crystal field levels. A_2^0 and A_2^2 are the crystal field coefficients introduced in Eq. (1), and $\langle r^n \rangle_{4f}$ is defined in Eq. (27), with $u^0 = u_{4f}^0(r)$. Within the framework of crystal field theory the thermal averages $\langle \cdots \rangle_T$ are known functions of the temperature once the crystal field parameters A_l^m are known, since the latter uniquely determine the crystal field levels.

The measurements of $\langle \Delta E \rangle_T$ were evaluated by two methods. In the first method the crystal field coefficients A_l^m were taken from optical spectroscopic data, while for $\langle r^n \rangle_{4f}$ theoretical estimates were used. In the second method no data other than $\langle \Delta E \rangle_T$ were used, in conjunction with a high-temperature expansion of the thermal averages $\langle \cdots \rangle_T$ in Eq. (34). The results obtained by the two methods were consistent. Table XV shows

TABLE XIV. Quadrupole polarizability of Tm^{3+} in a.u. $(0.5292\ \text{Å})^5$.

Excitation $nl_i \rightarrow l_f$	Variational principle	Numerical integration	Sternheimer numerical integration
$5s \rightarrow d$	4.91	4.54	2.89
$5p \rightarrow p$	3.64	3.38	3.09
$5p \rightarrow f$	12.68	15.44	11.46
$4s \rightarrow d$	0.02	0.03	0.02
$4p \rightarrow p$	0.01	0.01	0.01
$4p \rightarrow f$	0.04	0.04	0.02
$4d \rightarrow s$	0.02	0.02	0.01
$4d \rightarrow d$	0.03	0.03	0.02
$4d \rightarrow g$	0.07	0.07	0.04
Total	21.43	23.57	18.53

TABLE XV. Comparison of experimental data with theoretical values obtained in this work.

	Theoret. (this work)	Expt. Ref. 14	Expt. Ref. 14	Expt. Ref. 15	Expt. Ref. 15	Expt. Ref. 15.
	Tm^{3+}	TmES	Tm_2O_3	$TmRu_2$	$TmRe_2$	$TmMn_2$
$(1-\gamma_\infty)/(1-\sigma_2)$	154	250	130			
σ_2	0.577			0.57	0.58	0.64

the experimental results together with the theoretical values obtained in this work. The agreement for the intermetallic compounds is satisfactory, but for the ethylsulfate compound the agreement is bad. This corroborates the conclusions of Freeman and Watson[18] according to which covalency and overlap contributions play an important role in determining the energy spectrum of an ion, and the idea of an "isolated ion in a crystal field" does not describe the situation adequately in that particular crystal, even if shielding is taken into account. We believe, that the presently available Slater-modified Hartree-Fock wave functions for ions are adequate for the calculation of the shielding factors and quadrupole antishielding and polarization, if the numerical integration method is used, and the contribution from all shells is taken into account. (The calculation of shielding factors starting from the Dirac equation for relativistic wave functions is extremely complicated and has not yet been attempted.) Disagreement with experiment indicates, that the crystal field picture is inadequate for the crystal in question, and the combined effects of covalency, overlap and possibly nonlinear shielding may be estimated from the results of the comparison.

Neutron inelastic scattering experiments have been carried out on a series of praseodymium monochalcogenides and monopnictides.[19] These crystals have the NaCl structure, and the crystal field Hamiltonian of the Pr^{3+} ion in the $J=4$ multiplet may be written[20,21],

$$H_{cf} = A_4 \langle r^4 \rangle \beta_4 [O_4^0(4) + 5 O_4^4(4)] + A_6 \langle r^6 \rangle \gamma_4 [O_6^0(4) - 21 O_6^4(4)] .$$

Here O_n^m are the Stevens operator equivalents, β_4 and γ_4 are reduced matrix elements as tabulated by Hutchings.[22] The coefficients A_4 and A_6 are identical to A_4^0 and A_6^0, respectively. The experiments yield the energy differences of the lowest crystal field levels of the Pr^{3+} ion, from which $A_4 \langle r^4 \rangle$ and $A_6 \langle r^6 \rangle$ can be deduced. These are listed in Table XVI.

Similar values are obtained for Pr compounds of Bi, As, P, Te, Se, and S. Using the lattice constant $a = 6.376$ Å for PrSb, and unspecified values for $\langle r^4 \rangle$ and $\langle r^6 \rangle$ for Pr, the authors of Ref. 19 calculated the parameters listed in Table XVI.

TABLE XVI. Crystal field parameters in the chalcogenides PrSb and TmSb at the Pr and Tm ion sites. The values of $\langle r^n \rangle$ used for the theoretical estimates in the last two columns are taken from Table II, last column. For PrSb the effective charges $Z = \pm 2$ are used for Pr and Sb, respectively. For TmSb, Z is left as a parameter. Point charge crystal field model is used for the theoretical estimates. n. n. = six nearest neighbors only; data in meV.

		Expt. Refs. 19–21	Theoret. Refs. 19–21	This work n. n.	This work All ions
PrSb	$A_4\langle r^4 \rangle$	8.3 ± 0.3	8.4	8.50	8.89
PrSb	$A_6\langle r^6 \rangle$	0.17 ± 0.12	0.14	0.128	0.169
TmSb	$A_4\langle r^4 \rangle$	6.81 ± 0.10	$1.98Z$	$1.835Z$	$1.92Z$
TmSb	$A_6\langle r^6 \rangle$	0.44 ± 0.04	$0.022Z$	$0.0198Z$	$0.0262Z$

The calculations were done by a point charge nearest-neighbor model with an effective charge of -2.

There is an unexpectedly good agreement between the experimental and calculated values of these authors. Similar good agreement has been found for the other six compounds.

To check this result, we performed two calculations. In the first calculation we used the same model, as the authors of Ref. 19. In another model a sum is carried out over all the ions in the lattice, assigning $+2$ and -2 charges to the Pr and Sb ions, respectively. (For $+3$ and -3 charges the results should be multiplied by $\frac{3}{2}$.) In the nearest-neighbor point charge model the coefficients A_4 and A_6 are given by

$$A_4 = -14.4Z(14/a^5), \quad A_6 = -14.4Z(6/a^7)$$

if the charge Z is expressed in units of the electronic charge, a in Å, and the results for A_4 and A_6 in eV. Taking into account all ions, the formulas are

$$A_4 = -14.4Z2^{-6} \sum_i (35X_i^4 - 30X_i^2R_i^2 + 3R_i^4)/R_i^9 ,$$

$$A_6 = -14.4Z2^{-8} \tfrac{3}{2} \sum_i (231X_i^6 - 315X_i^4R_i^2 + 105X_i^2R_i^4 - 5R_i^6)/R_i^{13} ,$$

where X_i, Y_i, Z_i are the coordinates of the ions and $R_i = (X_i^2 + Y_i^2 + Z_i^2)^{1/2}$ and the sums are over all ions except the one at the coordinate origin. Using $\langle r^4 \rangle = 0.222$ Å^4, $\langle r^6 \rangle = 0.317$ Å^6, we obtain the set of results shown in Table XVI.

The agreement of our results with experiment is good for PrSb, but bad in TmSb. We tend to believe that the good agreement in the case of PrSb (as well as in the case of other Pr-chalcogenides and pnictides) is fortuitous, the more so, because the choice of $Z = 2$ effective charge on the Pr-ion to achieve this agreement is not readily justifiable. Once agreement has been forced for one compound, other isomorphic compounds will also conform because the crystal field coefficients scale with powers of the lattice constant.

ACKNOWLEDGMENTS

Our sincere thanks are due Dr. P. Rudra who devised the computer program for the numerical integration, to Dr. C. J. Lenander who provided us with a computer program to generate the unperturbed ionic wave function, and to Miss U. Wiese, who aided us in plotting the results.

APPENDIX A: ASYMPTOTIC BEHAVIOR OF WAVE FUNCTIONS AT $r = 0$

For our numerical solution of Eq. (28), the asymptotic behavior of the solution $u'(r)$ at $r = 0$ is of no importance. The function u' is given an arbitrary value at r_i (the closest point to $r = 0$, for which u^0 is known) and the integration proceeds outward. The correct value $u'(r_1)$ is determined by the asymptotic behavior of u' at $r \to \infty$ through iteration. In the numerical integrations necessary to find the shielding factors, $u'(r)$ is not used at any point r in the closed interval $(0, r_1)$.

In contrast to this, the asymptotic behavior of $u'(r)$ at $r = 0$ is important in the variational method. Here an analytic form of $u'(r)$ is used, and integrations are carried out analytically. To minimize the energy any series expansion of $u'(r)$ may be used (including positive and negative powers of r) as long as the energy expression, which is an integral over the wave function, is convergent. However, the use of such arbitrary series expansions for u' will not lead to correct values of the shielding parameters if u' has an incorrect asymptotic behavior at $r = 0$.

To determine the correct asymptotic behavior, let us set

$$u^0(l_i) = r^{l_i+1} \sum_{n=0}^{\infty} c_n r^n, \qquad c_0 \neq 0 \tag{A1}$$

$$u'(l_i \to l \to l_f) = r^{\alpha} \sum_{n=0}^{\infty} a_n r^n , \quad a_0 \neq 0 . \tag{A2}$$

The leading power l_{i+1} in (A1) reflects a well-known property of the Schrödinger equation with centrosymmetric potential. In (A2) the constant α is to be found.

Making use of the equation[8]

$$V_0 - E^0_{nl_i} = \frac{1}{u^0} \frac{d^2u^0(nl_i)}{dr^2} - \frac{l_i(l_i+1)}{r^2} = \frac{1}{r}(l_i+1)\frac{c_1}{c_0} + \sum_0^{\infty} d_n r^n , \tag{A3}$$

we conclude, by physical rather than mathematical reasoning, that $c_1 \neq 0$. This is so, because for small r the effective potential $V(r)$ must reduce to the Coulomb potential of the nucleus. The constants d_n are certain combinations of the constants which occur in (A1) and (A2). Setting

$$(c_1/c_0)(l_i+1) = d_{-1} \neq 0 , \tag{A4}$$

Eq. (31) may be written as follows for small r:

$$[-\alpha(\alpha-1)+l_f(l_f+1)]r^{\alpha-2}\sum_{n=0}^{\infty}a_n r^n + d_{-1}r^{\alpha-1} \times\sum_{n=0}^{\infty}a_n r^n - 2\alpha r^{\alpha-1}\sum_{n=1}^{\infty}n a_n r^{n-1} + r^{\alpha}\sum_{n=0}^{\infty}\sum_{m=0}^{\infty}d_n a_m r^{n+m} - \sum_{n=2}^{\infty}n(n-1)a_n r^{n-2} = (r^{l+l_i+1} - \delta_{l_i l_f} r^{l_i+1}\langle r^l\rangle)\sum_{n=0}^{\infty}c_n r^n . \quad \text{(A5)}$$

For *angular excitations* ($l_i \neq l_f$) there are two possibilities to explore. (i) In the first case we have

$$-\alpha(\alpha-1)+l_f(l_f+1)=0 ,$$

hence

$$\alpha = l_f + 1 .$$

In this case $r^{\alpha-1}$ is the lowest power of r on the left-hand side of (A5) with a nonvanishing coefficient, while on the right-hand side it is r^{l_i+l+1}. Consequently, we must have $\alpha = l_i + l + 2$. Since α is already determined, this leads to $l_f = l_i + l + 1$.

This condition cannot be fulfilled, since the angular parts of the wave function must also correspond on the two sides of the equation, which gives the condition

$$l_f = |l_i - l|, \ldots, |l_i + l| . \quad \text{(A6)}$$

Hence (i) is excluded.

(ii) The second possibility is

$$\alpha = l_f + 1.$$

Equating the lowest powers of r on both sides of (A5) yields

$$\alpha = l + l_i + 3. \quad \text{(A7)}$$

For *radial excitations* $l_f = l_i$ again there are two possibilities. (i) In the first case we have $-\alpha(\alpha-1)+l_f(l_f+1)=0$, hence $\alpha = l_f + 1$.

Equating lowest powers of r on both sides of (A5) leads to $\alpha = l_i + 2 = l_f + 2$, since $l_i = l_f$. This is a contradiction, and (i) is excluded.

(ii) The second possibility is

$$\alpha \neq l_i + 1.$$

Achievement of identical asymptotic behavior for $r = 0$ on both sides of (A5) now requires

$$\alpha = l_i + 3 . \quad \text{(A8)}$$

In summary, we arrive at the following variational wave function, written in terms of u^0:

$$u'(l_i \to l \to l_f ; r) = u^0(l_i ; r)\, r^{l+2}\sum_{n=0}^{\infty}a_n r^n \quad \text{for } l_i \neq l_f , \quad \text{(A9)}$$

$$u'(l_i \to l \to l_f ; r) = u^0(l_i ; r)(r^2\sum_{n=0}^{\infty}a_n r^n + f) \quad \text{for } l_i = l_f . \quad \text{(A10)}$$

Here, we have taken into account the fact, that for $l_f \neq l_i$ the homogeneous differential equation for $u(l_i \to l \to l_f)$ has no solution, because the constant $E^0_{l_i}$ which appears in the equation is not an eigenvalue. (The eigenvalue is $E^0_{l_f}$.) The homogeneous equation for $u'(l_i \to l \to l_i)$ has the solution $u^0(l_i)$, which, multiplied with a constant f has been added to the particular solution of the inhomogeneous equation.

APPENDIX B: VARIATIONAL CALCULATION OF QUADRUPOLE ANTISHIELDING FACTOR

Let us denote the type of integral which occurs in the quadrupole antishielding factor γ_∞ by

$$I_{pl}(l_i \to l_f) = \int r^p u^0(l_i)\, u'(l_i \to l \to l_f)\, dr . \quad \text{(B1)}$$

The function u' is obtained by minimizing the expression $\Phi_1 + \Phi_2$ with respect to the variational parameters a_n. The latter occur in the expansion

$$u'(l_i \to l \to l_f) = u^0(l_i) \quad \text{(B2)}$$

with

$$g(r) = \sum a_n r^n . \quad \text{(B3)}$$

Φ_1 and Φ_2 are given by

$$\Phi_1 = -2\int_0^\infty r^l u^0(l_i) u'(l_i \to l \to l_f)\, dr , \quad \text{(B4)}$$

$$\Phi_2 = \int_0^\infty u'(l_i \to l \to l_f)\left(\frac{d^2}{dr^2} + \frac{l_f(l_f+1)}{r^2} + V(r) - E_{l_i}\right) \times u'(l_i \to l \to l_f)\, dr . \quad \text{(B5)}$$

After some manipulations we obtain

$$\Phi_1 = -2\langle r^l g\rangle, \qquad \Phi_2 = \left\langle\left(\frac{dg}{dr}\right)^2\right\rangle + B(l_i; l_f)\langle r^{-2} g^2\rangle , \quad \text{(B6)}$$

with

$$B(l_i; l_f) = l_f(l_f+1) - l_i(l_i+1) . \quad \text{(B7)}$$

Making use of (B3) and (B6), the variational equations

$$\frac{\partial\Phi_1}{\partial a_n} + \frac{\partial\Phi_2}{\partial a_n} = 0 , \quad m = 0, \ldots, N \quad \text{(B8)}$$

may be written

$$\sum_{m=0}^{N} a_m [mn + B(l_i, l_f)]\langle r^{m+n-2}\rangle = \langle r^{l+n}\rangle, \quad n = 0, \ldots, N . \quad \text{(B9)}$$

The solution of this system of equations is

$$a_m = G_{mn}(l_i, l_f)\langle r^{l+n}\rangle, \quad m = 0, \ldots, N \quad \text{(B10)}$$

with

$$G^{-1}_{mn} = [mn + B(l_i, l_f)]\langle r^{m+n-2}\rangle . \quad \text{(B11)}$$

Note that

$$G_{mn} = G_{nm} . \quad \text{(B12)}$$

An important property of the matrix $G_{mn}(l_i, l_f)$ is that it does not depend on l. The only dependence

of a_m on l enters through the inhomogeneous term $\langle r^{l+n}\rangle$ of the set of Eqs. (B9).

Having determined a_m, hence $u'(l_i \to l \to l_f)$, from (B2) and (B3), we insert the result into (B1) and obtain

$$I_{pl}(l_i \to l_f) = \int [u^0(l_i)]^2 \sum_{mn} G_{mn} \langle r^{l+n}\rangle \langle r^{m+p}\rangle \, dr$$

$$= \sum_{mn} G_{mn}(l_i, l_f) \langle r^{l+n}\rangle \langle r^{m+p}\rangle \ . \qquad \text{(B13)}$$

From this and (B12) it follows that

$$I_{pl}(l_i \to l_f) = I_{lp}(l_i \to l_f) \ . \qquad \text{(B14)}$$

As a special case, for $l = 2$, $p = -3$ we obtain

$$\gamma_{\infty \text{ext}}(l_i \to 2 \to l_f) = \int r^{-3} u^0(l_i)\, u'(l_i \to 2 \to l_f)\, dr$$

$$= \int r^2 u^0(l_i)\, v'(l_i \to -3 \to l_f)\, dr$$

$$= \gamma_{\infty \text{nucl}}(l_i \to -3 \to l_f) \ . \qquad \text{(B15)}$$

This shows, that within the accuracy of the inversion routine for the matrix G^{-1} the external and nuclear quadrupole antishielding factors are equal. This has been verified by the numerical calculations.

---

*Research sponsored by the Air Force Office of Scientific Research, Office of Aerospace Research, United States Air Force, under AFOSR Grants Nos. 69-1745 and 70-1940.

†Work performed in partial fulfillment of the requirements for the M.S. degree. Present address: Department of Mining, Metallurgy, and Petroleum Engineering, University of Illinois, Urbana, Ill. 61801.

[1]This first estimate neglects the interpenetration of the charge distributions of the central and ligand ions, as well as some other effects discussed in Ref. 12.

[2]G. Burns, Phys. Rev. 128, 2121 (1962).

[3]R. M. Sternheimer, Phys. Rev. 146, 140 (1966).

[4]D. K. Ray, Proc. Phys. Soc. (London) 82, 47 (1963).

[5]R. M. Sternheimer, M. Blume, and R. F. Peierls, Phys. Rev. 173, 376 (1968).

[6]E. U. Condon and G. H. Shortley, *Theory of Atomic Spectra* (Cambridge U. P., London, 1935).

[7]R. A. Kromhout (private communication).

[8]R. M. Sternheimer, Phys. Rev. 96, 951 (1954).

[9]T. P. Das and R. Bersohn, Phys. Rev. 102, 733 (1956).

[10]E. C. Ridley, Proc. Cambridge Phil. Soc. 56, 41 (1960).

[11]C. J. Lenander, Phys. Rev. 130, 1033 (1963). We are particularly indebted to Dr. Lenander for his generosity in sending us his program and elucidating comments.

[12]D. Liberman, J. T. Waber, and D. T. Cromer, Phys. Rev. 137, A27 (1967).

[13]W. B. Lewis, LASL Report No. LA-DC-11574, 1970 (unpublished).

[14]R. G. Barnes, R. L. Mössbauer, E. Kankeleit, and J. M. Poindexter, Phys. Rev. 136, A175 (1964).

[15]D. L. Uhrich, D. J. Genin, and R. G. Barnes, Phys. Rev. 166, 261 (1968).

[16]G. Williams and L. L. Hirst, Phys. Rev. 185, 407 (1969).

[17]P. Junod, A. Menth, and O. Vogt, Phys. Letters 23, 626 (1966).

[18]A. J. Freeman and R. E. Watson, Phys. Rev. 135, A1209 (1964); 139, A1606 (1965); 156, 251 (1967).

[19]K. C. Turberfield, L. Passell, R. J. Birgeneau, and E. Bucher, Phys. Rev. Letters 25, 752 (1970).

[20]K. C. Turberfield *et al.*, J. Appl. Phys. 42, 1746 (1971).

[21]R. J. Birgeneau *et al.*, Phys. Rev. B 4, 718 (1971).

[22]M. T. Hutchings, in *Solid State Physics*, edited by F. Seitz and D. Turnbull (Academic, New York, 1964), Vol. 16.

[23]F. Herman and S. Skillman, *Atomic Structure Calculations* (Prentice-Hall, Englewood Cliffs, N. J., 1963).

[24]Complete tables of our calculations of the radial factor of the unperturbed wave functions of the Pr^{3+} and Tm^{3+} ions may be obtained by ordering document NAPS 01894 from ASIS-National Auxiliary Publications Service, c/o CCM Information Corp., 866 Third Ave., New York, N. Y. 10022, remitting $2.00 for each microfiche or $5.00 for each photocopy.